# Mechanism of Flavin Reduction in the Class 1A Dihydroorotate Dehydrogenase from *Lactococcus lactis*†

Rebecca L. Fagan,‡ Kaj Frank Jensen,§ Olof Björnberg,§,|| and Bruce A. Palfey*,‡

*Department of Biological Chemistry, University of Michigan Medical School, Ann Arbor, Michigan 48109-0606, and Institute of Molecular Biology, University of Copenhagen, DK-1307 Copenhagen K, Denmark*

*Received November 29, 2006; Revised Manuscript Received January 12, 2007*

ABSTRACT: Dihydroorotate dehydrogenases (DHODs) oxidize dihydroorotate (DHO) to orotate (OA) using the FMN prosthetic group to abstract a hydride equivalent from C6 and a protein residue (cysteine for class 1A DHODs) to deprotonate C5. The fundamental question of whether the scission of the two DHO C−H bonds is concerted or stepwise was addressed for the class 1A enzyme from *Lactococcus lactis* by determining kinetic isotope effects (KIEs) on flavin reduction in anaerobic stopped-flow experiments. Isotope effects were determined at two pH values. At pH 7.0, KIEs were ∼2-fold for DHO labeled singly at the 5-position or the 6-position and ∼4-fold for DHO labeled at both the 5- and 6-positions. At pH 8.5, the KIEs observed for DHO labeled at the 5-position, the 6-position, and the 5- and 6-positions were ∼2-, ∼3-, and ∼6-fold, respectively. These isotope effects are consistent with a concerted oxidation of DHO. The pH dependence of reduction was also determined, and a p$K_a$ of 8.3 was found. This p$K_a$ can be attributed to the ionization of the active site cysteine which deprotonates C5 of DHO during the reaction. To further investigate the importance of the active site base, two site-directed mutants were also studied: Cys130Ala (removal of the active site base) and Cys130Ser (replacement with the active site base used by class 2 DHODs). Both mutant enzymes exhibited binding affinities for DHO similar to that of the wild-type enzyme. Reduction of both mutants was extremely slow compared to that of the wild type; the rate of reduction increased with pH, showing no sign of a plateau. Interestingly, double-deuterium isotope effects on the Cys130Ser mutant also showed a concerted mechanism for flavin reduction.

Dihydroorotate dehydrogenase (DHOD)[1] is a flavin-containing enzyme that catalyzes the only redox reaction in the pyrimidine biosynthetic pathway, the conversion of dihydroorotate (DHO) to orotate (OA; Scheme 1). DHODs have been categorized into two broad classes based on sequence, class 1 and class 2 (*1*). Class 2 DHODs are membrane-bound proteins. This class of enzymes uses serine as an active site base and is oxidized by ubiquinone (*2*). Class 1 DHODs, in comparison, are cytosolic proteins which contain cysteine as their active site base. This class of enzymes has been further divided into two subclasses. Class 1A enzymes are homodimers that are oxidized by fumarate (*3*). Class 1B enzymes are $\alpha_2\beta_2$ heterotetramers, which contain not only FMN (like all other DHODs) but also an iron−sulfur cluster and FAD, where the enzyme is oxidized by NAD (*4*).

Several pathogens, including *Enterococcus faecalis* and *Trypanosoma cruzi*, express class 1A DHODs, while humans have class 2 enzymes, making class 1A DHODs inviting drug targets. Genetic studies have shown that DHOD is essential for the survival of *T. cruzi* (*5*), validating the idea that inhibitors specific for class 1A enzymes could treat diseases. Most DHOD inhibitors discovered to date are directed at the hydrophobic quinone binding pocket found in class 2 DHODs, not the pyrimidine binding site (*6*). Class 1A DHODs, however, do not have a quinone binding pocket to target. Specifically targeting the pyrimidine binding site of class 1A DHODs would appear to be difficult because the structure of the pyrimidine binding site in class 1A and class 2 DHODs is nearly identical (*7*−*9*). However, functional rather than structural differences between the pyrimidine binding sites may exist that could be exploited in drug design. Thus, determining the differences between the mechanisms utilized by these classes of enzymes should aid in the design of class-specific inhibitors.

Scheme 1

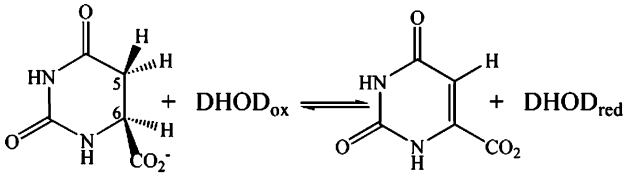


In all classes of DHODs, DHO is converted to OA by breaking two C−H bonds. The reaction involves both a

† This work was supported by NIH Grant GM61087. R.L.F. was supported by NIGMS Training Grant GM07767.

* To whom correspondence should be addressed. Phone: (734) 615-2452. Fax: (734) 763-4581. E-mail: brupalf@umich.edu.

‡ University of Michigan Medical School.

§ University of Copenhagen.

|| Present address: Department of Cell and Organism Biology, Lund University, S-223 62 Lund, Sweden.

[1] Abbreviations: DHOD, dihydroorotate dehydrogenase; DHO, dihydroorotate; OA, orotate; KIE, kinetic isotope effect; $KP_i$, potassium phosphate buffer.

10.1021/bi602460n CCC: $37.00 
Published on Web 03/07/2007

deprotonation and a hydride transfer. During the oxidation of DHO, the C5 *pro-S* hydrogen of DHO (*10*) is removed by an active site base, either cysteine in class 1 enzymes or serine in class 2 enzymes. The hydrogen on C6 of DHO is transferred to N5 of the isoalloxazine of the flavin as a hydride or hydride equivalent. The oxidation of DHO to OA could occur via a concerted mechanism, where both C−H bonds break simultaneously, or a stepwise mechanism, where the C−H bonds break sequentially. Double kinetic isotope effects (KIEs) can determine which mechanism is operational. Class 2 DHODs from *Escherichia coli* and *Homo sapiens* have been previously studied in stopped-flow experiments. With those enzymes, the KIEs suggested either a stepwise mechanism or a concerted mechanism with quantum mechanical tunneling (*11*). In this paper, we examine the class 1A enzyme from *Lactococcus lactis* and find that the oxidation of DHO by this enzyme is concerted and the active site cysteine acts as a classic general base.

## EXPERIMENTAL PROCEDURES

*Overexpression and Purification of DHODs.* Wild-type *L. lactis* DHOD, the Cys130Ser mutant, and the Cys130Ala mutant were expressed from the pFN1 plasmid (*1, 12*). The enzymes were expressed in SØ6645 cells as previously described (*12*). The cells overexpressing the proteins were harvested by centrifugation (4000 rpm for 25 min at 4 °C). Enzyme was purified either according to the published procedure (*12*) or by the following method. Cells were resuspended in 20 mM Bis-Tris buffer (pH 6.5) containing 10% glycerol and lysed by sonication, and the cell debris was removed by centrifugation at 16 000 rpm for 20 min at 4 °C. Addition of 50% ammonium sulfate (313 g/L) to the cleared lysate precipitated proteins other than the recombinantly expressed DHOD. Precipitated proteins were removed by centrifugation at 16 000 rpm for 20 min at 4 °C. The bright yellow supernatant containing the enzyme was dialyzed overnight in 3 L of 20 mM Bis-Tris buffer (pH 6.5) containing 10% glycerol to remove the salt. The dialyzed enzyme was then filtered with a 0.45 $\mu$m syringe filter and applied to a Q-Sepharose fast-flow resin (Sigma-Aldrich) previously equilibrated in 20 mM Bis-Tris buffer (pH 6.5) containing 10% glycerol. The enzyme was eluted with a linear gradient from 0 to 500 mM NaCl in 20 mM Bis-Tris buffer (pH 6.5) containing 10% glycerol. The fractions containing enzyme were pooled, concentrated, and stored at −80 °C after being diluted with glycerol to 50% (v/v). For use in experiments, the enzyme was exchanged into the appropriate buffer using Econo-Pac 10DG disposable desalting columns (Bio-Rad).

*Synthesis of Deuterium-Labeled DHO.* Deuterium-labeled DHO was synthesized from L-dihydroorotic acid (Sigma) or orotic acid (Aldrich) according to the procedures of Pascal and Walsh (*13*) and characterized by $^1$H NMR (Supporting Information). Synthetic DHOs were found to be >94% isotopically pure.

*Instrumentation.* Absorbance spectra were obtained using a Shimadzu UV-2501PC scanning spectrophotometer. Stopped-flow experiments were performed at 4 °C using a Hi-Tech Scientific KinetAsyst SF-61 DX2 stopped-flow spectrophotometer.

*Preparation of Anaerobic Solutions.* Enzyme solutions for rapid reaction studies were made anaerobic in glass tonometers by repeated cycles of evacuation and equilibration over an atmosphere of purified argon as previously described (*14*). Substrate solutions were made anaerobic within the syringes that were to be loaded onto the stopped-flow instrument by bubbling solutions with purified argon. Slow reactions were performed in anaerobic cuvettes (*15*) and monitored in a standard scanning spectrophotometer. These reaction mixtures were also made anaerobic by repeated evacuation and equilibration with purified argon.

*pH Dependence of the Reduction of Wild-Type DHOD from L. lactis.* The pH dependence of the reductive half-reaction of wild-type DHOD from *L. lactis* was studied from pH 6.47 to 10.36 (MOPS from pH 6.47 to 7.96, TAPS at pH 8.58, and CHES from pH 9.3 to 10.36). The anaerobic enzyme equilibrated in the buffer of interest (50 mM buffer adjusted to an ionic strength of 50 mM with KCl) was mixed with various concentrations of DHO (up to 8 mM before mixing) in the same buffer. Reaction traces were collected at both 475 and 550 nm. Kinetic traces were fit to either two or three exponentials with Program A (R. Chang, C.-J. Chiu, J. Dinverno, and D. P. Ballou, University of Michigan). The reduction rate constant ($k_{red}$) was determined from the limiting value of the observed rate constant at an infinite DHO concentration obtained by fitting $k_{obs}$ versus DHO concentration to a hyperbola in Kaleidagraph (Synergy, Inc.). The p$K_a$ value controlling reduction was determined by fitting the pH dependence of the reduction rate constant to eq 1

$$k_{red} = \frac{k_{red,limiting}}{1 + 10^{pK_a - pH}} \quad (1)$$

where $k_{red,limiting}$ is the limiting value of the reduction rate constant at high pH.

*Identification of Spectral Intermediates.* Anaerobic enzyme equilibrated in 100 mM Tris-HCl and 0.1 mM EDTA (pH 8.5) was mixed with 4 mM DHO in the same buffer. Absorbance spectra were collected from 350 to 700 nm for 0.4 s with an integration time of 1.5 ms using a diode-array detector. Absorbance spectra of intermediates were calculated in SpecFit/32 (Spectrum Software Associates) via singular-value decomposition using a two-step model. Anaerobic enzyme was mixed with buffer containing no DHO to obtain the spectrum of the fully oxidized enzyme.

*Kinetic Isotope Effects in Wild-Type DHOD.* Double deuterium isotope effects were measured at pH 7.0 and 8.5. Anaerobic enzyme equilibrated in the buffer of interest (either 40 mM KPi at pH 7.0 or 50 mM Tris at pH 8.5) was mixed with various concentrations (up to 8 mM before mixing) of labeled and unlabeled DHO. Reaction traces were collected at 475 and 550 nm, and $k_{red}$ values were determined as described above. KIEs were calculated by dividing the $k_{red}$ determined for protio-DHO by the $k_{red}$ determined for each labeled substrate.

*Binding of DHO to the Cys130Ala and Cys130Ser Mutants.* The reductive half-reaction of the Cys130Ala mutant was excruciatingly slow, allowing the direct aerobic titration of the enzyme with DHO to determine a dissociation constant. The enzyme equilibrated in the buffer of interest was titrated with DHO in the same buffer. The buffers used for this pH dependence were the same as those described for wild-type reduction experiments. After the titration was complete, the titration mixture was filtered (Centricon 30)

to remove enzyme and the extent of reaction was determined from the orotate concentration in the filtrate ($\epsilon_{280} = 7.52$ $mM^{-1}$ $cm^{-1}$). In the time course of an experiment (~30 min), the reaction had not proceeded to an appreciable extent (<5%). The reductive half-reaction of the Cys130Ser mutant was faster than that of the Cys130Ala mutant. Therefore, aerobic titrations for this mutant were performed in the stopped-flow spectrophotometer, allowing spectra to be scanned within 10 s of mixing. For both mutants, the differences in flavin absorbance caused by binding of DHO were plotted against DHO concentration, and the data were fit to a hyperbola in Kaleidagraph (Synergy, Inc.) to determine the $K_d$.

*Dependence of pH on the Reductive Half-Reactions of Cys130Ala and Cys130Ser.* In the active site base mutants, flavin reduction did not occur on a stopped-flow time scale; therefore, all reductive half-reactions were assessed using a standard scanning spectrophotometer under anaerobic conditions at pH values ranging from 6.47 to 10.36. Anaerobic enzyme equilibrated in a particular buffer (same buffers used for the pH dependence of the reduction of the wild-type enzyme) was mixed with a saturating concentration of DHO (from 2 to 10 mM; always $\geq 10K_d$), and spectra were recorded at intervals until flavin reduction was complete. Since flavin reduction was extremely slow in the Cys130Ala mutant, reduction reactions were performed at 25 °C. For the Cys130Ser mutant, reduction reactions were performed at 4 °C to facilitate comparison with the wild type. Reduction rate constants were determined by fitting the absorbance traces at 475 nm to either one or two exponentials. Since a saturating DHO concentration was used in each experiment, the $k_{obs}$ obtained from fitting the exponential traces is equivalent to $k_{red}$.

*Kinetic Isotope Effects on Flavin Reduction in the Cys130Ser Mutant.* Deuterium isotope effects were also determined for the Cys130Ser mutant. The extremely slow rate of the Cys130Ala mutant prevented the determination of KIEs for this mutant. Anaerobic Cys130Ser DHOD in 50 mM TAPS (50 mM ionic strength, pH 8.5, 4 °C) was mixed with 3 mM substrate (either labeled or unlabeled), and spectra were recorded at intervals until flavin reduction was complete. Kinetic traces at 475 nm were fit to a single exponential to give $k_{red}$. Reduction with each substrate was repeated a minimum of three times, and the $k_{red}$ values that were obtained were averaged. The averaged $k_{red}$ values were used to determine the KIE by dividing the $k_{red}$ calculated for protio-DHO by the $k_{red}$ calculated for each labeled substrate.

## RESULTS

*Reduction of the Class 1A DHOD.* Our goal was to determine the mechanism of reduction of FMN by DHO. Stopped-flow methods provide the most direct window for observing this chemistry because large spectral changes accompany the reaction. Often, steady-state kinetics are used to address such questions, but in an enzyme as complex as DHOD, the reduction could be obscured by other processes. The catalytic cycle of DHOD consists of two half-reactions. In the reductive half-reaction, the focus of this study, the enzyme-bound flavin is reduced by DHO. In the oxidative half-reaction, the reduced enzyme is oxidized by fumarate. Reactions other than flavin reduction, such as fumarate reduction or product dissociation, could be partly or completely rate-determining in turnover, masking the chemistry of interest. Therefore, rather than study the mechanism in the steady state, we elected to study flavin reduction directly by only observing the reductive half-reaction, the conversion of DHO to OA and concomitant reduction of the enzyme.

The reductive half-reaction of the class 1A DHOD from *L. lactis* was studied by mixing the anaerobic oxidized enzyme with anaerobic DHO in the absence of an oxidizing substrate. All experiments were conducted at 4 °C to sufficiently slow the reaction so it could be observed. Absorbance spectra were collected using a diode-array detector from 350 to 700 nm over the course of 0.4 s (Figure 1A). Singular-value decomposition indicated one reaction intermediate; therefore, data were fit to a two-step model to calculate spectra. DHO binds to the enzyme in the dead time of the stopped-flow instrument causing a large red shift in flavin absorbance (Figure 1B). This shift in the flavin peak (from 456 to 475 nm) seen in the enzyme−substrate complex is similar to that previously observed for DHOD−DHO complexes in the class 2 enzymes from *E. coli* (*16*) and *H. sapiens* (*11*). After formation of the enzyme−substrate complex, flavin absorbance at 475 nm decreases rapidly as DHO is oxidized. The reduced enzyme−OA complex formed in this reaction has a charge-transfer band extending to long wavelengths, which indicates stacking of OA with the reduced FMN. This is seen as an increase in absorbance at 550 nm (Figure 1B). This charge-transfer band is also observed in class 2 DHODs (*16*). The charge-transfer absorbance of the reduced enzyme is lost upon product dissociation, producing the spectrum of the reduced enzyme (Figure 1B).[2]

Rate constants for the reductive half-reaction were determined from absorbance traces at either 475 or 550 nm. At 475 nm, a large decrease in absorbance representing flavin reduction is followed by a small decrease in absorbance representing product dissociation (Figure 1C). At 550 nm, flavin reduction is accompanied by an increase in absorbance while OA dissociation is seen as a decrease in absorbance (Figure 1C). Rate constants for both flavin reduction and product dissociation were determined by fitting to sums of exponentials. At either wavelength, the observed rate constant of the first phase, representing flavin reduction, varied hyperbolically with DHO concentration, allowing the rate constant for flavin reduction ($k_{red}$) and the $K_d$ to be determined. At pH 8.5 and 4 °C, the $k_{red}$ was $157 \pm 4$ $s^{-1}$ and the $K_d$ was $240 \pm 30$ $\mu$M. The rate constant of charge-transfer disappearance was $25 \pm 2$ $s^{-1}$. Sometimes, a final small phase was observed that showed no concentration dependence. It is not clear what this phase represents, but we speculate that it was caused by the consumption of a small amount of contaminating oxygen. Regardless of its origin, this reaction phase was well-resolved, always being at least 1 order of magnitude slower than product release.

[2] Occasionally, the enzyme did not fully reduce in the time frame of a stopped-flow experiment, but instead stopped with half of the oxidized flavin remaining. The origin of this apparent half-sites reactivity in the homodimeric enzyme is not known but has been observed previously (*17*, *18*). Regardless of whether the enzyme was reduced completely or only halfway, the rate constants and spectral changes were identical.

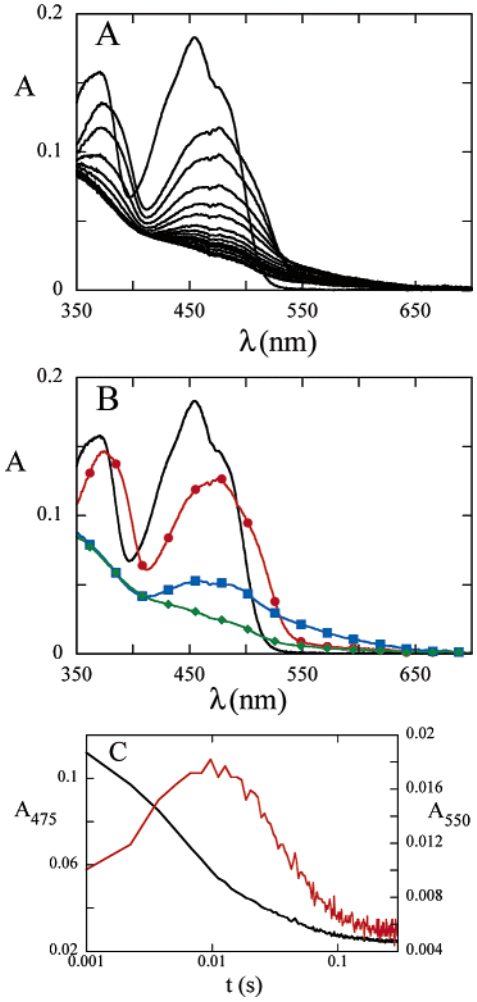


FIGURE 1: Spectral changes during reduction. (A) Anaerobic DHOD (15.9 $\mu$M after mixing) was mixed with DHO (2 mM after mixing) in 0.1 M Tris-HCl and 0.1 mM EDTA (pH 8.5) at 4 °C in a stopped-flow spectrophotometer, and spectra were collected with a diode array over 0.4 s. The starting spectrum of fully oxidized DHOD was collected by mixing anaerobic DHOD with anaerobic buffer. (B) Intermediates were calculated from the data in panel A by singular-value decomposition and fitting to a two-step model in SpecFit (Spectrum Software Associates). The spectrum of oxidized DHOD is colored black. A large red shift in flavin absorbance is seen in the Michaelis complex (red), which reacts to yield the reduced enzyme−product complex having a charge-transfer band extending to long wavelengths (blue). OA dissociation gives an enzyme with the final spectrum (green). (C) Single-wavelength data from panel A are plotted as a function of time. At 475 nm (black), the peak of the Michaelis complex, a biphasic decrease in flavin absorbance is seen. At 550 nm (red), flavin reduction is seen as an increase in absorbance followed by a decrease caused by OA dissociation. Note that time is on a logarithmic scale.

*pH Dependence of the Reductive Half-Reaction.* The reductive half-reaction of *L. lactis* DHOD was studied from pH 6.47 to 10.36 in anaerobic stopped-flow experiments. The enzyme at the pH of the experiment was mixed with various concentrations of DHO at the same pH. During the course of these experiments, it was noticed that higher ionic strengths increased the observed rates of reduction (data not shown), consistent with previously published data that showed a higher ionic strength favored increased activity in this enzyme (*19*). Because of this, all buffers used to determine the pH dependence had a constant ionic strength of 50 mM. At each pH, the observed rate constant for

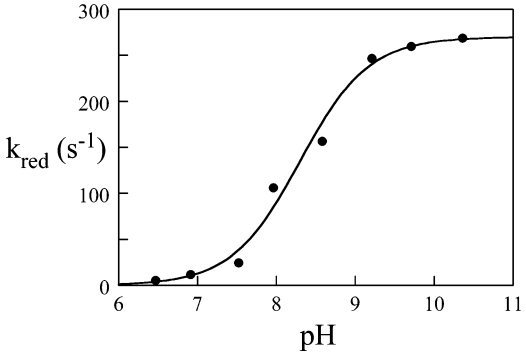


FIGURE 2: pH dependence of reduction of the wild type. The limiting rate constants for reduction ($k_{red}$) were obtained from stopped-flow experiments at 4 °C as described in the text. The plot was fit to eq 1, giving a p$K_a$ value of 8.3 ± 0.1 and a maximum rate constant for flavin reduction at high pH of 270 ± 10 $s^{-1}$.

reduction varied hyperbolically with DHO concentration, allowing the determination of both the reduction rate constant and the $K_d$ of DHO. The reduction rate constant increased with pH until reaching a limiting value of 270 ± 10 $s^{-1}$ (Figure 2). The pH profile gave a p$K_a$ controlling reduction of 8.3 ± 0.1. This p$K_a$ is consistent with crystal structures which indicate that the active site base is Cys130. The $K_d$ of DHO (~200 $\mu$M) was essentially independent of pH until pH 9, whereupon it increased with pH showing no sign of a plateau, reaching a value of 1 mM at the highest pH value that was studied, 10.36. The loss of affinity of DHO at high pH could be due to the deprotonation of N3 of DHO or lysine 43 (which makes a salt bridge to the pyrimidine in the crystal structure) (*7*). The rate constant for dissociation of the product from the reduced enzyme (loss of charge-transfer absorbance) varied randomly between 22 and 35 $s^{-1}$ at all pH values studied above 7.5. Below pH 7.5, the rate of flavin reduction was slower than 22 $s^{-1}$, changing the rate-limiting step of the overall reaction from product release to flavin reduction, preventing the observation of the charge-transfer complex.

*Active Site Base Mutants.* The importance of the active site base in the reduction of DHOD was investigated by studying the reactions of Cys130Ala (where the active site base is removed) and Cys130Ser (where the active site base is replaced with the active site base utilized in class 2 DHODs). Reduction of the flavin was very slow in both mutants; however, the binding of DHO to both mutants caused an immediate red shift in the flavin absorbance as seen in the wild type. The slow reaction allowed the $K_d$ of DHO to be determined by direct aerobic titration for the Cys130Ala mutant, as the extent of reaction over the course of the titration was negligible. In this mutant, the $K_d$ of DHO (~200 $\mu$M) was unaffected by pH until a pH of 9.35 was reached. A maximum $K_d$ value of ~400 $\mu$M was found at pH 10.22, the highest pH evaluated. To determine the $K_d$ of DHO for the Cys130Ser mutant, aerobic DHO titrations were performed in the stopped-flow spectrophotometer, allowing spectra to be scanned within 10 s of mixing. Similar to that of the wild-type enzyme, the $K_d$ of DHO in the Cys130Ser mutant remained around 200 $\mu$M until pH 9 was reached. At that point, the $K_d$ increased with no sign of plateau to a maximum value of 600 $\mu$M at pH 10.3, the highest pH value that was investigated.

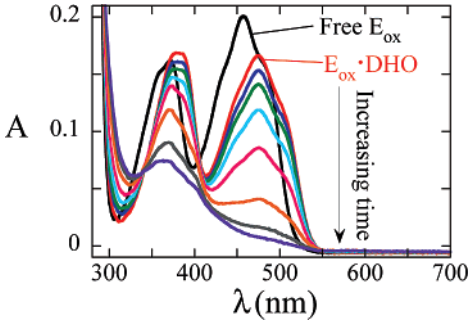


FIGURE 3: Reduction of the Cys130Ser mutant. DHO (10.4 $\mu$L, 250 mM) was added to 1.29 mL of 16.7 $\mu$M Cys130Ser in 50 mM MOPS (50 mM ionic strength, pH 7.5, 4 °C) in an anaerobic cuvette. Immediately upon mixing, the flavin absorbance undergoes a red shift from 456 to 475 nm (red) as seen in the wild-type enzyme. Flavin absorbance then decreases slowly with time. For clarity, only selected spectra are shown. As the reaction proceeds, anionic semiquinone was produced, as evidenced by peaks and shoulders at 370 and 400 nm (prominent in the orange and gray spectra). The final spectrum was taken 44 h after mixing.

Scheme 2

$$DHOD_{ox} + DHO \longrightarrow DHOD_{ox}{\bullet}DHO \longrightarrow DHOD_{red}{\bullet}OA \longrightarrow DHOD_{red} + OA$$

$$DHOD_{ox}{\bullet}DHO + DHOD_{red}\ (\pm\ DHO) \longrightarrow 2\ Semiquinone\ (\pm\ DHO)$$

The reductive half-reaction of both mutants was studied at saturating DHO concentrations ($\geq 10K_d$). Upon addition of DHO, the flavin absorption peak immediately shifted from 456 to 475 nm as seen in the wild-type enzyme (Figure 3). Slow flavin reduction was observed following addition of DHO. No charge-transfer complex was observed because the rate of product release is not changed by the active site base mutation; however, the rate of reduction is significantly reduced, preventing the accumulation of the charge-transfer complex.

During the course of reduction, both mutant enzymes formed anionic semiquinone as evidenced by peaks and shoulders at 370 and 400 nm (Figure 3). The semiquinone produced during the reduction was ultimately consumed, however, at a very slow rate, requiring several days, and therefore reactions were not routinely followed to completion. In some cases, the kinetic traces at 475 nm fit to a single exponential, while in other cases, the traces required an extra phase for good fits. In those cases, the two observed rates were close, differing by only ~3-fold, with the second phase apparently related to semiquinone reduction. It is not clear why this phase is not always resolved, but semiquinone was always detected. Semiquinone production required the presence of DHO. Simply reducing the enzyme in the absence of DHO with a xanthine/xanthine oxidase reducing system (*20*) or dithionite did not produce semiquinone (Supporting Information). Furthermore, using DHO concentrations in vast excess of the $K_d$ (100 times) resolved the reaction traces into two phases without changing the observed rate constant of the first phase, suggesting that differential binding of DHO to the semiquinone and reduced forms of the enzyme changes their reactivities. Our data suggest that following two-electron reduction, the hydroquinone reacts with the unreacted oxidized enzyme forming semiquinone (Scheme 2). This could occur by several conceivable intra- and intermolecular mechanisms. A detailed dissection of these findings is beyond the scope of this work.

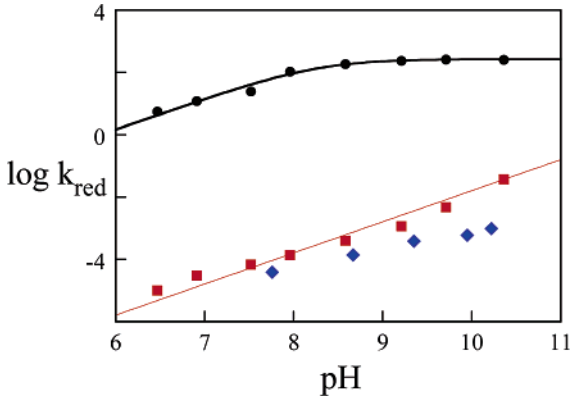


FIGURE 4: pH dependence of reduction of Cys130Ser and Cys130Ala mutants. The limiting rate constants for reduction ($k_{red}$) of the Cys130Ser mutant (red squares) were obtained at 4 °C as described in the text and Figure 3; those for the Cys130Ala mutant (blue diamonds) were obtained at 25 °C. Neither mutant shows an accessible p$K_a$ in the pH range that was investigated, and both mutants were reduced extremely slowly. The pH dependence of the wild-type enzyme, previously shown in Figure 2, is also shown in this figure (black circles) for comparison.

The effect of pH on the reduction rate constant of the Cys130Ser mutant was studied at saturating DHO concentrations at 4 °C. The rate constant increased with pH from $9.9 \times 10^{-6}$ s$^{-1}$ at pH 6.47 to 0.03 s$^{-1}$ at pH 10.36 (Figure 4) but did not show a p$K_a$. The rate of reduction observed with the Cys130Ser mutant was 4 orders of magnitude lower than the rate obtained using wild-type DHOD at pH 10.36, and the difference between the rates was even larger at lower pH values.

The pH dependence on the reduction of the Cys130Ala mutant was also studied. This reaction was even slower than that of the Cys130Ser mutant, so rate constants were determined at 25 °C instead of 4 °C using saturating DHO concentrations ($\geq 10K_d$). Below pH 7.7, the protein was not stable and would precipitate after ~20 h, preventing the determination of the rate constant for reduction. From pH 7.7 to 10.2, the rate constant increased from $3.8 \times 10^{-5}$ to $9.6 \times 10^{-4}$ s$^{-1}$ but never reached an accessible p$K_a$ (Figure 4).

*Kinetic Isotope Effects.* The oxidation of DHO could occur by either a concerted or a stepwise mechanism. To determine which mechanism is utilized by the wild-type class 1A DHOD from *L. lactis*, kinetic isotope effect experiments were conducted using DHO labeled at either the 5-position, the 6-position, or both the 5- and 6-positions. Absorbance traces at 475 nm (Figure 5) were fit to three exponentials. The fast phase, corresponding to flavin reduction, varied hyperbolically with DHO concentration, allowing the rate constant for reduction to be determined. Kinetic isotope effects (KIEs) were obtained by dividing the $k_{red}$ determined for protio-DHO by the $k_{red}$ determined for deuterated DHO.

KIEs were determined for the wild-type enzyme at pH 7.0 and 8.5. At pH 7.0, using [5,5-$^2H_2$]DHO, a KIE of 1.83 ± 0.04 was found (Table 1), and a KIE of 2.21 ± 0.04 was obtained using [6-$^2$H]DHO. The double KIE determined using [5,5,6-$^2H_3$]DHO was found to be 4.3 ± 0.2. The KIE values obtained at pH 8.5 using [5,5-$^2H_2$]DHO, [6-$^2$H]DHO,

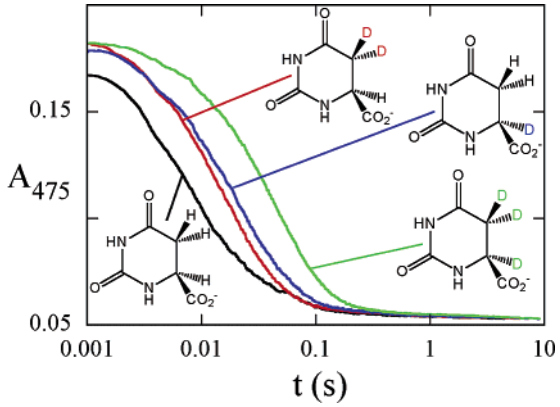


FIGURE 5: Reduction of the wild type with labeled and unlabeled DHO. Anaerobic DHOD (final concentration of 15 $\mu$M) was mixed with anaerobic substrate (final concentration of 2 mM) at pH 8.5. Note that the reaction traces (475 nm) are shown on a logarithmic time scale. The spectrum of protio-DHO is colored black, that of [5,5-$^2H_2$]DHO red, that of [6-$^2$H]DHO blue, and that of [5,5,6-$^2H_3$]-DHO green. The traces were adjusted by adding a constant to matching final absorbance.

Table 1: Reduction Rate Constants and KIEs for the Wild Type[a]

| | pH 7.0 | | pH 8.5 | |
|---|---|---|---|---|
| compound | $k_{red}$ ($s^{-1}$) | KIE | $k_{red}$ ($s^{-1}$) | KIE |
| DHO | 12.0 ± 0.1 | | 164 ± 3 | |
| [5,5-$^2H_2$]DHO | 6.5 ± 0.1 | 1.83 ± 0.04 | 73 ± 2 | 2.2 ± 0.1 |
| [6-$^2$H]DHO | 5.44 ± 0.06 | 2.21 ± 0.04 | 57 ± 2 | 2.9 ± 0.1 |
| [5,5,6-$^2H_3$]DHO | 2.77 ± 0.08 | 4.3 ± 0.2 | 28.3 ± 0.3 | 5.8 ± 0.3 |

[a] The $k_{red}$ values used to calculate the KIE were obtained from the value at a saturating DHO concentration as explained in Experimental Procedures. The highest concentration of DHO used was 4 mM after mixing (~20$K_d$).

and [5,5,6-$^2H_3$]DHO were 2.2 ± 0.1, 2.9 ± 0.1, and 5.8 ± 0.3, respectively.

Double deuterium isotope effects were also used to study the mechanism of DHO oxidation in the *L. lactis* Cys130Ser mutant DHOD.[3] Anaerobic Cys130Ser DHOD was mixed with saturating concentrations (≥10$K_d$) of labeled and unlabeled substrate as described in Experimental Procedures. Kinetic traces at 475 nm (Figure 6) were fit to a single exponential to give $k_{red}$ values. At pH 8.5, KIE values of 2.56 ± 0.14, 1.65 ± 0.13, and 4.57 ± 0.58 were obtained for DHO deuterated at the 5-position, 6-position, and 5- and 6-positions, respectively (Table 2).

## DISCUSSION

DHODs are flavin-containing enzymes that catalyze the oxidation of DHO to OA with the concomitant reduction of the FMN prosthetic group. We studied the mechanism of flavin reduction in the class 1A DHOD from *L. lactis* in detail, looking at the pH dependence of reduction as well as the double kinetic isotope effects associated with DHO oxidation. To further investigate the importance of the active site base, two base mutants were also studied: Cys130Ala (where the active site base has been removed) and Cys130Ser

[3] Isotope effect experiments were not conducted with the Cys130Ala mutant due to the extremely slow rate of flavin reduction.

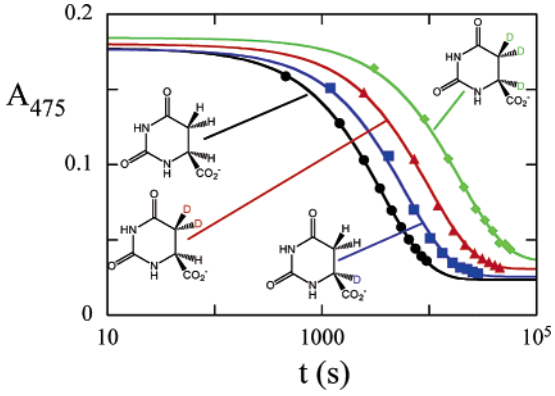


FIGURE 6: Reduction of the Cys130Ser mutant with labeled and unlabeled DHO. Anaerobic DHOD (final concentration of 15 $\mu$M) was mixed with anaerobic substrate (final concentration of 3 mM) at 4 °C in a scanning spectrophotometer at pH 8.5, and spectra were scanned at intervals as in Figure 3. Absorbance traces at 475 nm were extracted from the data and fit to single exponentials to obtain rate constants. The spectrum of protio-DHO is colored black, that of [5,5-$^2H_2$]DHO red, that of [6-$^2$H]DHO blue, and that of [5,5,6-$^2H_3$]DHO green. Most points were omitted for clarity; the curves are the fits to the complete data set. Note that time is on a logarithmic scale.

Table 2: Reduction Rate Constants and KIEs for the Cys130Ser Mutant at pH 8.5[a]

| compound | $k_{red}$ ($s^{-1}$) | KIE |
|---|---|---|
| DHO | $2.61 \times 10^{-4} \pm 9 \times 10^{-6}$ | |
| [5,5-$^2H_2$]DHO | $1.02 \times 10^{-4} \pm 2 \times 10^{-6}$ | 2.56 ± 0.14 |
| [6-$^2$H]DHO | $1.58 \times 10^{-4} \pm 7 \times 10^{-6}$ | 1.65 ± 0.13 |
| [5,5,6-$^2H_3$]DHO | $5.71 \times 10^{-5} \pm 5.3 \times 10^{-6}$ | 4.57 ± 0.58 |

[a] The $k_{red}$ values used to calculate the KIE were determined by averaging values from fits of at least three separate traces obtained at saturating (≥10$K_d$) DHO concentrations at 4 °C; reported errors are the standard deviations on the averaged rate constants.

(where the active site base has been switched to the base utilized in class 2 DHODs).

When DHO binds to the wild-type class 1A DHOD, the flavin absorbance undergoes a dramatic red shift. Similar red shifts are seen for the binding of several ligands to all oxidized DHODs that were investigated. Substrates, such as DHO or dihydrooxonate, products, such as orotate or oxonate, or nonreactive inhibitors, such as 3,5-dihydroxybenzoate, cause this red shift upon binding (*16*, *18*, *21*). Spectra of flavoproteins often undergo large shifts when reaction intermediates are formed (*22*). However, this red-shifted spectrum is not that of a chemical intermediate, because products and inhibitors give the same shift but cannot react with oxidized enzyme. In addition, the same shift was observed instantly in the nearly unreactive mutants. Binding of a ligand to flavoproteins often causes charge-transfer bands (*22*). However, the red shift cannot be the formation of charge-transfer absorbance because charge-transfer transitions require an electron-rich donor to be in contact with the electron-deficient flavin, but the binding of electron-poor ligands such as OA causes the red shift. It is possible that the proximity of the dipole of the ligands to the flavin causes this shift. It is not surprising that this shift occurs in all classes of DHODs, given the very similar structures of the active sites in these enzymes. Both classes of DHODs contain four highly conserved asparagine residues (*7*−*9*) that have been shown to interact with OA in the product complex crystal

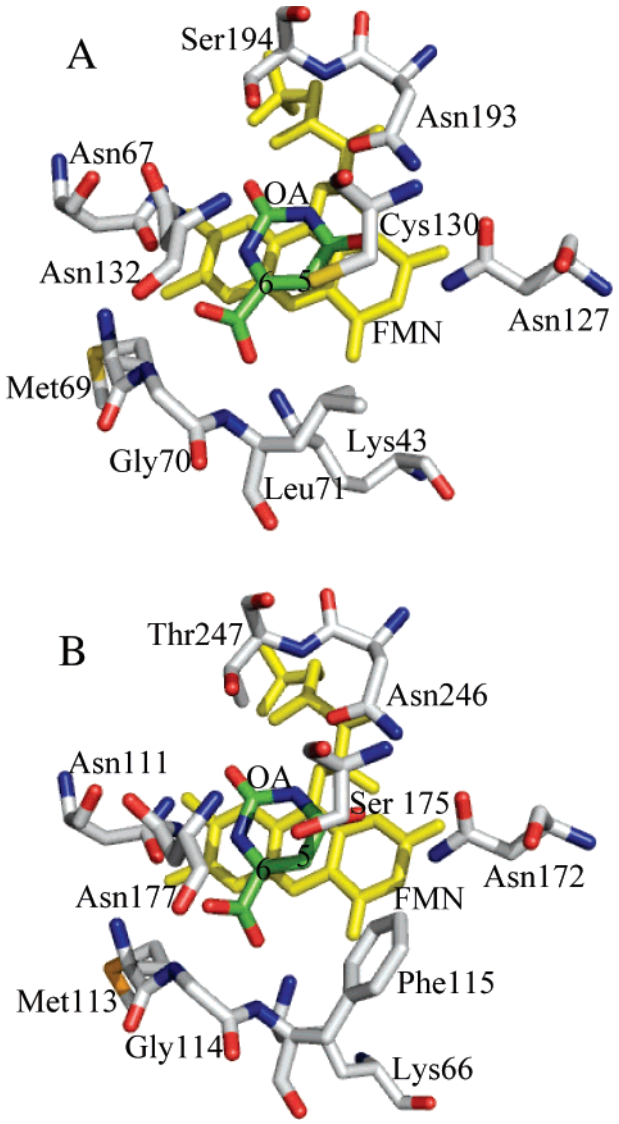


FIGURE 7: Pyrimidine binding pockets of DHODs. The flavin, OA, and key active site residues are shown for the class 1A enzyme from *L. lactis* (A) and the class 2 enzyme from *E. coli* (B). Note the similar OA−protein interactions, the proximities of the active site bases to the 5-position of OA, and the propinquities of the 6-position of OA to N5 of FMN in both structures. Coordinates were taken from PDB entries 2dor and 1f76.

structures, and the remainder of the active site is also nearly identical in the two classes of enzymes (Figure 7).

The rate of flavin reduction is pH-dependent in the class 1A DHOD from *L. lactis*. In this enzyme, cysteine 130 is acting as a general base to deprotonate C5 of DHO. The p$K_a$ controlling reduction (~8.3) is similar to that of unperturbed cysteine, suggesting that the cysteine is not activated by other active site residues. This is expected from crystal structures, which show nothing in the active site that would activate the cysteine. Our finding is also consistent with previously published work that used chemical modification to investigate the p$K_a$ of this enzyme (*1*). When the active site base was mutated to either Ala or Ser, the originally observed p$K_a$ (~8.3) is no longer observed, providing further evidence of the assignment of the p$K_a$ to residue Cys130. The lack of an observable p$K_a$ in the Cys130Ser mutant is consistent with our conclusion that the active site does not provide large electrostatic perturbations

Table 3: Analysis of KIEs

| | [5,5-$^2H_2$]DHO | [6-$^2$H]DHO | predicted double KIEs[a] | [5,5,6-$^2H_3$]DHO |
|---|---|---|---|---|
| | | *L. lactis* Wild Type | | |
| pH 7.0 | 1.83 ± 0.04 | 2.21 ± 0.04 | 4.0 ± 0.2 | 4.3 ± 0.2 |
| pH 8.5 | 2.2 ± 0.1 | 2.9 ± 0.1 | 6.5 ± 0.6 | 5.8 ± 0.3 |
| | | Cys130Ser | | |
| pH 8.5 | 2.56 ± 0.14 | 1.65 ± 0.13 | 4.22 ± 0.56 | 4.57 ± 0.58 |

[a] The rule of the geometric mean predicts that the double KIE equals the product of each single KIE if the reaction occurs in a single transition state (*23*).

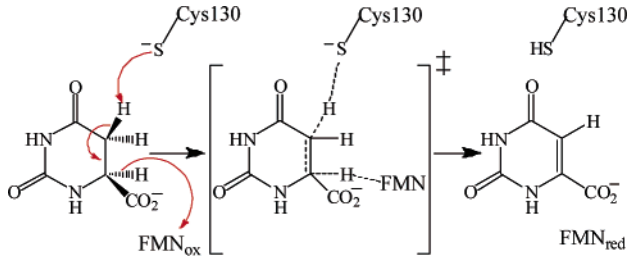


FIGURE 8: Mechanism of DHO oxidation by the class 1A DHOD from *L. lactis*. The conversion of DHO to OA occurs via a single transition state in which the active site base, cysteine, deprotonates DHO as the hydride is transferred to the flavin.

to lower the p$K_a$ of the base. Serine has a p$K_a$ of 13.6 in aqueous solution (*23*). If the enzyme had lowered the p$K_a$ by ~3 units or more, the shift would have been detected.

The oxidation of DHO requires the deprotonation of the *pro-S* hydrogen on C5 of DHO and the transfer of the C6 hydrogen to the flavin as a hydride or hydride equivalent. The reaction could occur either by a concerted mechanism (both C−H bonds break at the same time) or by a stepwise mechanism (the C−H bonds break sequentially). Double kinetic isotope effects can be used to distinguish between concerted or stepwise mechanisms for flavin reduction. The rule of the geometric mean states that in the absence of large quantum effects, perturbations to a partition function caused by isotopic substitutions at a particular site are independent of isotopic substitutions at another site (*24*). Therefore, if both C−H bonds break in a concerted mechanism (i.e., a single transition state), then the product of the two single isotope effects, obtained by multiplying the KIEs obtained with [5,5-$^2H_2$]DHO and [6-$^2$H]DHO, will equal the observed double KIE, obtained with [5,5,6-$^2H_3$]DHO. At both pH values that were investigated, the rule of the geometric mean is obeyed within experimental error (Table 3). This rules out major tunneling effects, and we conclude that the oxidation of DHO by the class 1A DHOD from *L. lactis* is concerted (Figure 8).

The question of whether the flavin of DHOD is reduced in a concerted or stepwise mechanism has been addressed previously for the class 1A enzyme from *Crithidia fasciculata* (*13*). In contrast to our work, that study concluded that DHO oxidation was stepwise, based on a steady-state kinetic analysis of multiple deuterium isotope effects. We offer two possible explanations for these different conclusions. First, it is possible that there is variation of the reaction mechanisms within class 1A DHODs. However, all other biochemical properties of DHODs segregate according to the phylogenetic classification. Alternatively, the different con-

clusions could have a chemical rationale. At the time the steady-state analysis was performed, class 1A DHODs had not yet been shown to use fumarate as the oxidizing substrate and dissolved oxygen was used instead. Most reduced flavoenzymes will reduce $O_2$ even if it is not the physiological substrate; its reaction with DHOD does not require the participation of an active site acid. The bimolecular rate constant observed for the oxidation of the Cys130Ser mutant by $O_2$ is nearly identical to that of the wild type (B. A. Palfey, unpublished data). The rate of exchange of the protons derived from DHO between a reduced class 1A enzyme and solvent has been shown to be slow relative to catalysis (*24*). Thus, when oxygen rather than fumarate is used as the oxidizing substrate, the active site cysteine, which acted as a base in the reductive half-reaction, will very likely remain protonated or deuterated after flavin oxidation. It must be deprotonated prior to the next turnover with DHO, and a significant isotope effect can be expected because fractionation factors of thiols are generally ~0.5 or less (*25*). Therefore, in steady-state kinetics using $O_2$ as the oxidizing substrate, isotope effects from deprotonation of the active site cysteine could also contribute to the observed isotope effects. Such a possibility was not considered.

Changing the active site base did not alter the concerted mechanism. The Cys130Ser DHOD mutant obeyed the rule of the geometric mean (Table 3) just as the wild type. The class 2 DHODs from *E. coli* and *H. sapiens* do not obey the rule of the geometric mean, leading to the conclusion that class 2 DHODs utilize either a stepwise mechanism or a concerted mechanism with significant quantum mechanical tunneling (*11*). Therefore, the identity of the active site base is not responsible for the difference in mechanism between the two classes despite the otherwise nearly identical active site structures (Figure 7). Subtle dynamic features may be in play in these two classes of enzymes that determine the mechanism of DHO oxidation.

The value of the KIE for deprotonating DHO barely increased when the active site cysteine was mutated to serine (Table 3), suggesting that the extent of proton transfer did not change markedly between the two transition states. However, the value of the KIE for hydride transfer decreased ~2-fold due to the mutation, indicating a lower extent of hydride transfer in the transition state of the mutant enzyme. The different KIEs, measured under the same conditions, clearly indicate changes in transition-state structures between the wild-type and mutant enzymes, although the mechanism of DHO oxidation is concerted in both enzymes.

We have detected a significant difference in the mechanisms of the two classes of DHODs, but the basis of this difference is not yet clear. The measurement of other isotope effects, such as heavy atom effects, should allow the structures of the different transition states to be deduced. Differences in transition-state structures might open the possibility of designing class-specific inhibitors for various DHODs.

## SUPPORTING INFORMATION AVAILABLE

$^1$H NMR spectra of labeled DHO and anaerobic reduction experiments with ligand-free Cys130Ser. This material is available free of charge via the Internet at http://pubs.acs.org.

## REFERENCES


1. Björnberg, O., Rowland, P., Larsen, S., and Jensen, K. F. (1997) Active site of dihydroorotate dehydrogenase A from *Lactococcus lactis* investigated by chemical modification and mutagenesis, *Biochemistry 36*, 16197−16205.
2. Jones, M. E. (1980) Pyrimidine nucleotide biosynthesis in animals: Genes, enzymes, and regulation of ump biosynthesis, *Annu. Rev. Biochem. 49*, 253−279.
3. Nagy, M., Lacroute, F., and Thomas, D. (1992) Divergent evolution of pyrimidine biosynthesis between anaerobic and aerobic yeasts, *Proc. Natl. Acad. Sci. U.S.A. 89*, 8966−8970.
4. Nielsen, F. S., Andersen, P. S., and Jensen, K. F. (1996) The B form of dihydroorotate dehydrogenase from *Lactococcus lactis* consists of two different subunits, encoded by the pyrDB and pyrK genes, and contains FMN, FAD, and [FeS] redox centers, *J. Biol. Chem. 271*, 29359−29365.
5. Annoura, T., Nara, T., Makiuchi, T., Hashimoto, T., and Aoki, T. (2005) The origin of dihydroorotate dehydrogenase genes of kinetoplastids, with special reference to their biological significance and adaptation to anaerobic, parasitic conditions, *J. Mol. Evol. 60*, 113−127.
6. Palfey, B. A., Björnberg, O., and Jensen, K. F. (2001) Specific inhibition of a family 1A dihydroorotate dehydrogenase by benzoate pyrimidine analogues, *J. Med. Chem. 44*, 2861−2864.
7. Rowland, P., Björnberg, O., Nielsen, F. S., Jensen, K. F., and Larsen, S. (1998) The crystal structure of *Lactococcus lactis* dihydroorotate dehydrogenase A complexed with the enzyme reaction product throws light on its enzymatic function, *Protein Sci. 7*, 1269−1279.
8. Nørager, S., Jensen, K. F., Björnberg, O., and Larsen, S. (2002) *E. coli* dihydroorotate dehydrogenase reveals structural and functional distinctions between different classes of dihydroorotate dehydrogenases, *Structure 10*, 1211−1223.
9. Liu, S., Neidhardt, E. A., Grossman, T. H., Ocain, T., and Clardy, J. (2000) Structures of human dihydroorotate dehydrogenase in complex with antiproliferative agents, *Structure 8*, 25−33.
10. Blattmann, P., and Retey, J. (1972) Stereospecificity of the dihydroorotate-dehydrogenase reaction, *Eur. J. Biochem. 30*, 130−137.
11. Fagan, R. L., Nelson, M. N., Pagano, P. M., and Palfey, B. A. (2006) Mechanism of flavin reduction in class 2 dihydroorotate dehydrogenases, *Biochemistry 45*, 14926−14932.
12. Nielsen, F. S., Rowland, P., Larsen, S., and Jensen, K. F. (1996) Purification and characterization of dihydroorotate dehydrogenase A from *Lactococcus lactis*, crystallization and preliminary X-ray diffraction studies of the enzyme, *Protein Sci. 5*, 852−856.
13. Pascal, R. A., Jr., and Walsh, C. T. (1984) Mechanistic studies with deuterated dihydroorotates on the dihydroorotate oxidase from *Crithidia fasciculata*, *Biochemistry 23*, 2745−2752.
14. Palfey, B. A. (2003) Time resolved spectral analysis, in *Kinetic analysis of macromolecules* (Johnson, K. A., Ed.) pp 203−227, Oxford University Press, New York.
15. Williams, C. H., Jr., Arscott, L. D., Matthews, R. G., Thorpe, C., and Wilkinson, K. D. (1979) Methodology employed for anaerobic spectrophotometric titrations and for computer-assisted data analysis, *Methods Enzymol. 62*, 185−198.
16. Palfey, B. A., Björnberg, O., and Jensen, K. F. (2001) Insight into the chemistry of flavin reduction and oxidation in *Escherichia coli* dihydroorotate dehydrogenase obtained by rapid reaction studies, *Biochemistry 40*, 4381−4390.
17. Shi, J., Dertouzos, J., Gafni, A., Steel, D., and Palfey, B. A. (2006) Single-molecule kinetics reveals signatures of half-sites reactivity in dihydroorotate dehydrogenase A catalysis, *Proc. Natl. Acad. Sci. U.S.A. 103*, 5775−5780.
18. Nørager, S., Arent, S., Björnberg, O., Ottosen, M., Lo Leggio, L., Jensen, K. F., and Larsen, S. (2003) *Lactococcus lactis* dihydroorotate dehydrogenase A mutants reveal important facets of the enzymatic function, *J. Biol. Chem. 278*, 28812−28822.
19. Ottosen, M. B., Björnberg, O., Nørager, S., Larsen, S., Palfey, B. A., and Jensen, K. F. (2002) The dimeric dihydroorotate dehydrogenase A from *Lactococcus lactis* dissociates reversibly into inactive monomers, *Protein Sci. 11*, 2575−2583.
20. Massey, V. (1990) in *Flavins and Flavoproteins* (Curti, B., Ronchi, S., and Zanetti, G., Eds.) pp 59−66, Walter de Gruyter, Berlin.

21. Björnberg, O., Jordan, D. B., Palfey, B. A., and Jensen, K. F. (2001) Dihydrooxonate is a substrate of dihydroorotate dehydrogenase (DHOD) providing evidence for involvement of cysteine and serine residues in base catalysis, *Arch. Biochem. Biophys. 391*, 286−294.
22. Palfey, B. A., and Massey, V. (1998) Flavin-dependent enzymes, in *Comprehensive biological catalysis, volume iii: Radical reactions and oxidation/reduction* (Sinnott, N., Ed.) pp 83−154, Academic Press, New York.
23. Bruice, T. C., Fife, T. H., Bruno, J. J., and Brandon, N. E. (1962) Hydroxyl group catalysis. II. The reactivity of the hydroxyl group of serine. The nucleophilicity of alcohols and the ease of hydrolysis of their acetyl esters as related to their pKa, *Biochemistry 1*, 7−12.
24. Bigelisen, J. (1955) Statistical mechanics of isotope systems with small quantum corrections. I. General considerations and the rule of the geometric mean, *J. Chem. Phys. 23*, 2264−2267.
25. Cleland, W. W. (1980) Measurement of Isotope Effects by the Equilibrium Perturbation Technique, *Methods Enzymol. 64*, 104−125.

BI602460N